THE JOURNAL OF PHYSICAL CHEMISTRY A

Article

pubs.acs.org/JPCA

Ab Initio Studies of Calcium Carbonate Hydration

Josue A. Lopez-Berganza,[†] Yijue Diao,[†] Sudhakar Pamidighantam,[‡] and Rosa M. Espinosa-Marzal*[,†]

[†]Smart Interfaces in Environmental Nanotechnology, Civil and Environmental Engineering, University of Illinois at Urbana−Champaign, 205 North Matthews Avenue, Urbana, Illinois 61801, United States

[‡]Science Gateways Group, Research Technologies, UITS, Indiana University, 2709 East 10th Street, Bloomington, Indiana 47408, United States

Supporting Information

ABSTRACT: Ab initio simulations of large hydrated calcium carbonate clusters are challenging due to the existence of multiple local energy minima. Extensive conformational searches around hydrated calcium carbonate clusters ($CaCO_3{\cdot}nH_2O$ for n = 1−18) were performed to find low-energy hydration structures using an efficient combination of Monte Carlo searches, density-functional tight binding (DFTB +) method, and density-functional theory (DFT) at the B3LYP level, or Møller−Plesset perturbation theory at the MP2 level. This multilevel optimization yields several low-energy structures for hydrated calcium carbonate. Structural and energetics analysis of the hydration of these clusters revealed a first hydration shell composed of 12 water molecules. Bond-length and charge densities were also determined for different cluster sizes. The solvation of calcium carbonate in bulk water was investigated by placing the explicitly solvated $CaCO_3{\cdot}nH_2O$ clusters in a polarizable continuum model (PCM). The findings of this study provide new insights into the energetics and structure of hydrated calcium carbonate and contribute to the understanding of mechanisms where calcium carbonate formation or dissolution is of relevance.

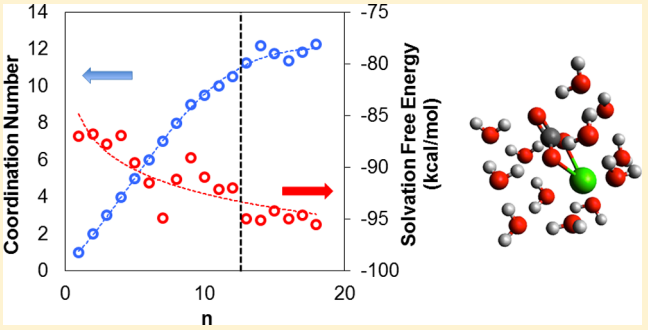

INTRODUCTION

Calcium carbonate is ubiquitous in nature; it is found in fresh and saline waters, soils, sediments, mineral dusts, and geologic formations.[1] Knowledge of the precipitation and dissolution mechanisms of calcium carbonate is of fundamental importance to many fields. For example, the life of many organisms relies on their ability to synthesize calcium carbonate[2,3] (i.e., a process called biomineralization), which is the main constituent of their strong and tough protective shells.[4−6] Calcium carbonate precipitation is one of the most important mechanisms for geological CO_2 sequestration, and it shows promise as a method for prevention of migration of CO_2 and drilling fluids in wellbores.[1,7,8] Microbiologically induced precipitation of calcium carbonate has been also proposed as a method for toxic metal treatment in contaminated environments.[9] Besides, various technological problems may arise from scale formation, such as drinking water distribution pipe blockages and fouling of desalination membranes.[10]

Hydrated ions in solution (Ca^{2+}, and CO_3^{2-}; HCO_3^- is not of relevance in the pH range of 9 to 10 that is considered here[11,12]) interact through electrostatic forces and hydrogen bonding between the respective hydration shells.[13] As a result, a few inner-shell water molecules are released, which increases the entropy of the system, and a common hydration shell forms. As the hydration shell regulates the mobility of the ion pairs in solution, and the interaction with other ion pairs, it affects calcium carbonate precipitation already at the very early stages, during the formation of prenucleation clusters (PNC), i.e. noncrystalline association of hydrated ions.[3,14] Computational studies show that the densification and dehydration of PNCs into dense liquid nanodroplets and amorphous calcium carbonate (ACC) is critically dependent on the state of the hydration of the interacting ions.[11,13,15−18]

The hydration shell of Ca^{2+} has been thoroughly characterized experimentally and computationally. The reported first-shell coordination number ranges from 4 to 10 water molecules.[13,19,20] On average, Ca^{2+} coordinates 6 water molecules in its first hydration shell.[21] The average binding energy of the water molecules decreases monotonically as the hydration shell becomes larger.[7,10] There are several experimental limitations for the study of the hydration shell of CO_3^{2-}. Among these, a narrow pH range is needed to prevent the predominance of bicarbonate ions at pH < 9.[13,22] First-shell coordination numbers of 7−12 water molecules have been previously reported for CO_3^{2-}.[13,23−25]

The solvation of a single calcium carbonate was studied by Bruneval et al. using gas-phase Molecular Dynamics (MD) simulations.[23] This study revealed a structured and anisotropic first hydration shell of a bidentate structural motif, in which there are five preferred sites for the water molecules interacting

Received: September 15, 2015
Revised: October 26, 2015
Published: October 27, 2015

DOI: 10.1021/acs.jpca.5b09006
J. Phys. Chem. A 2015, 119, 11591−11600

with Ca^{2+}. Each of the two CO_3^{2-} oxygen atoms closer to calcium (Mid-O_c in Figure 1) forms two hydrogen bonds with

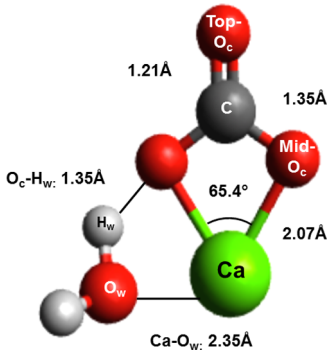

Figure 1. Calcium carbonate with one water molecule optimized at the B3LYP/6-311G(d,p) level. Calcium (green), carbon (gray), oxygen (red), hydrogen (white).

water. The carbonate oxygen farthest to calcium (Top-O_c in Figure 1) can form up to four hydrogen bonds with water. Hydrophobic regions above and below the CO_3^{2-} ion were observed in the hydration layers. These hydrophobic sites could potentially play a role in the formation of ikaite, the hydrated form of calcium carbonate which has a structure characterized by stacked CO_3^{2-}.[23]

Ab initio quantum chemistry simulations have been successfully applied to study the hydration shell of ions in aqueous systems and to parametrize MD force fields.[11,26−28] Ab initio simulations consider clusters consisting of varying number of water molecules surrounding the ion. The reliability and accuracy of these simulations is partially limited by the number of water molecules (n) because large clusters ($n > 5$) become increasingly complex and have a large number of local minima on the potential energy surface.[29] Although traditional MD simulations can consider much larger systems and lead to a correct estimation of thermodynamic quantities *if* appropriate force fields are assumed, ab initio studies are of interest because they do not require assumption of force fields and empirical parameters. The accuracy of the force fields for alkaline-Earth carbonate systems is still in debate. Unreliable predictions of the thermodynamics and kinetics of calcium carbonate by MD simulations can originate from inconsistent force fields; a new force field for alkaline-earth carbonate systems has been recently proposed,[30] whereas the need of proper water potentials has been also highlighted in this work. In this regard, we note that reactive potentials that allow water dissociation can be essential for MD simulations.[31] The results from ab initio static calculations are often used to parametrize interactions through a potential function.[23,32−34] Combinations of MD and ab initio static calculations have been also reported. For example, Di Tommaso and de Leeuw performed Car−Parrinello MD of calcium carbonate and water, but they used DFT static calculations—instead of DFT MD—to explore the structure and energetics of the microsolvated clusters of calcium bicarbonate with an increasing number of water molecules.[35] They argued that although Car−Parrinello DFT MD can explicitly take into account the electronic structure and enable the accurate modeling of many-body and polarization effects, it is difficult to perform simulations large enough to yield *thermodynamic averages* owing to computational limitations. Here we present a Monte Carlo-based exploration of the configuration space for water and calcium carbonate clusters of specific size that provides an alternative to a time evolution analysis by Car−Parrinello MD simulations. Determining the energetics of hydrated clusters of different size, i.e. composed of a different number of water molecules, is of relevance for elucidating the mineralization path of calcium carbonate, as various hydration states of calcium carbonate are expected during nucleation and growth, i.e. a (partial) dehydration. For the reasons mentioned above, we have performed an ab initio static study of both the structural details of hydrated calcium carbonate clusters with a variable number of water molecules and their thermodynamic stability.

Extensive conformational searches are needed to generate reliable equilibrium structures that can translate ab initio calculations on small clusters to bulk solvation energies.[29] Zhao et al.[29] implemented a computationally efficient method to perform conformational searches on large clusters ($n = 8$) using a combination of Monte Carlo searches and a density-functional-based tight-binding method (DFTB+). This approach was successful in combining the speed of the Monte Carlo searches to generate structures and the accuracy of higher-level computational methods, such as DFTB+, for energy calculations. Inspired by this approach, this paper implements multilevel conformational searches of large calcium carbonate and water clusters with a maximum of 18 water molecules and performs ab initio-level calculations to provide insight into the structure and the thermodynamics of the hydration shell of a single calcium carbonate molecule, which is the first building unit in the precipitation pathway of calcium carbonate. To the best of our knowledge, a structural and thermodynamic analysis of this scale on the hydration shell of calcium carbonate has not been carried out yet.

We note here that HCO_3^- was not investigated in our simulations. This choice is based on the usual basic solution condition for synthesis of ACC,[2,36] which drives the equilibrium toward CO_3^{2-}. Additionally, NMR experimental studies have shown HCO_3^- to be absent in the final ACC structure.[11,12] Although we do not explicitly consider pH in the discussed simulations, the basic conditions are implicit through the use of carbonate.

■ COMPUTATIONAL METHODS

Multiple configurations of a cluster consisting of a single calcium carbonate molecule surrounded by n water molecules, $CaCO_3 + nH_2O$, n ranging from 1 to 18, were generated with the Monte Carlo module in TINKER (version 6.3.3)[37] to identify equilibrium structures. First, the free energy of the cluster was calculated with the selected force fields (OPLS-AA and MMFF) for the estimated geometry. Then, a Monte Carlo move was applied to achieve a new configuration, whose energy was also calculated. Configurations with higher strain energies were discarded. If the energy of the new configuration was smaller than the previous one, the geometry was saved, and the Monte Carlo move was repeated until the convergence criterion was satisfied, or the maximum number of steps (20,000) was reached. Each Monte Carlo move was restricted to be smaller than 3 Å RMS distance from the previous one. An RMS gradient of 0.01 kcal/mol/Å for the strain energy was used as a convergence criterion. It is to note that force fields specific to calcium carbonate (see e.g.[15−18,23,30,33,38,39]) were not needed here, as the force fields were only used to generate candidate structures that were further optimized by more rigorous ab initio methods as described below. Thus, the final

DOI: 10.1021/acs.jpca.5b09006
J. Phys. Chem. A 2015, 119, 11591−11600

structures and energetics reported in our work are the result of ab initio optimizations, i.e. they do not rely on the assumption of a force field, in contrast to common MD force fields.

Each of the geometries generated by TINKER was further optimized by a density-functional-based tight-binding (DFTB) semiempirical procedure using the DFTB+ software (Version 1.2),[40] and a tight-binding energy minimization approach. The self-consistent charge (SCC) tight binding parameters were set to a tolerance of 10^{-10} electrons and a maximum of 1000 cycles. A modified Anderson charge mixing method available in DFTB + packages was utilized for convergence acceleration.[41] Calcium was assigned a d Slater orbital; carbon and oxygen were given p Slater orbitals, and the hydrogens used an s-type orbital. Parameters used in these simulations were obtained from a recently published 3OB_parametrization set for alkaline earth metals that includes calcium.[42]

After optimizing each conformation with DFTB+, the two lowest-energy configurations were further optimized by density functional theory (DFT) methods using Gaussian09 software.[43] The hybrid density functional B3LYP and a 6-311+G (d,p) basis set were selected. Additionally, the lowest energy structures from each TINKER Monte Carlo set of calcium carbonate clusters ($CaCO_3{\cdot}nH_2O$) were optimized at the DFT level. Geometrical optimization were performed and vibrational frequencies were obtained for each structure at room temperature. Optimized structures with imaginary frequencies were discarded. The molecular charge distribution of the calcium carbonate in each cluster was obtained using the Natural Bond Orbital analysis,[44] which provides a more accurate description of electron distribution compared to the default Mulliken charges available in Gaussian09.[45]

Hydration of calcium carbonate by n water molecules was modeled by optimizing the structure of a single calcium carbonate molecule with n water molecules (n = 1−18):

$$CaCO_3 + nH_2O \rightarrow CaCO_3{\cdot}nH_2O$$

Møller−Plesset perturbation theory at second-order (MP2)[46] with a basis set of 6-311+G(d,p) was used to independently verify the structural and relative energies of hydrated structures obtained by DFT.

The solvation free energies of calcium carbonate and the effects of bulk water were investigated using the polarizable continuum model (PCM) and the integral equation formalism variant (IEFPCM) in Gaussian09. The clusters were placed in a cavity surrounded by water as a solvent (continuum) to simulate aqueous conditions. The solvation free energy $\Delta G^{*\mathrm{CaCO3}}_{\mathrm{solv}}$ is obtained from the thermodynamic cycle shown in Figure 2 on the basis of refs 35,47

$$\Delta G^{*\mathrm{CaCO_3}}_{\mathrm{solv}} = \Delta G^{\mathrm{CaCO_3}{\cdot}n\mathrm{H_2O}}_{\mathrm{clust}} + \Delta G^{*\mathrm{CaCO_3}{\cdot}n\mathrm{H_2O}}_{\mathrm{gl}} + n\Delta G^{\mathrm{H_2O}}_{\mathrm{vap}}$$

where $\Delta G^{\mathrm{CaCO_3}{\cdot}n\mathrm{H_2O}}_{\mathrm{clust}}$ is the free energy of formation of the gas-phase cluster, which is obtained from the free energy difference between the gas-phase cluster and its components and is calculated by ab initio. $\Delta G^{*\mathrm{CaCO_3}{\cdot}n\mathrm{H_2O}}_{\mathrm{gl}}$ is the free energy of the hydrated cluster from gas to liquid corresponding to 1 mol/L and obtained from the ab initio free energy difference between the gas-phase cluster and the solvated cluster. $\Delta G^{\mathrm{H_2O}}_{\mathrm{vap}}$ is the vaporization free energy of a single water molecule[35] and is obtained from

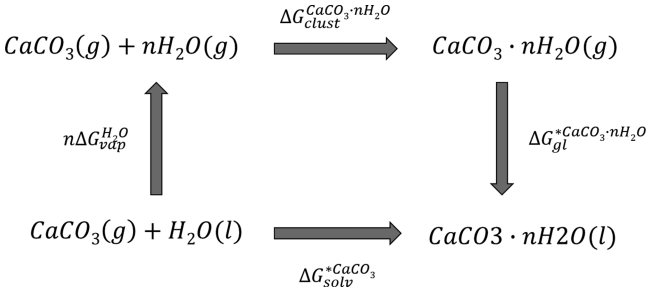

Figure 2. Thermodynamic cycle to determine the solvation free energy of calcium carbonate $\Delta G^{*\mathrm{CaCO_3}}_{\mathrm{solv}}$ via vaporization of water $\Delta G^{\mathrm{H_2O}}_{\mathrm{vap}}$, the free energy of the hydrated cluster from gas to liquid phase $\Delta G^{*\mathrm{CaCO_3}{\cdot}n\mathrm{H_2O}}_{\mathrm{gl}}$, and the free energy of formation of the gas-phase cluster $\Delta G^{\mathrm{CaCO_3}{\cdot}n\mathrm{H_2O}}_{\mathrm{clust}}$.

$$\Delta G^{\mathrm{H_2O}}_{\mathrm{vap}} = -\Delta G^{*\mathrm{H_2O}}_{\mathrm{solv}} - RT\ln(\tilde{R}\mathrm{T}) - RT\ln\left[\frac{[\mathrm{H_2O}]}{\frac{1\ \mathrm{mol}}{\mathrm{L}}}\right]$$

where $\tilde{R}$ = 0.082053 K^{-1}, $[H_2O]$ = 55.5 mol/L, and $\Delta G^{*\mathrm{H_2O}}_{\mathrm{solv}}$ = −5.05 kcal/mol is the solvation free energy of water, according to the PCM model.[35,47] The quality of this method is validated by comparing calculated solvation free energies of Ca^{2+} and Mg^{2+}, $\Delta G^{*\mathrm{Ca^{2+}}}_{\mathrm{solv}}$ and $\Delta G^{*\mathrm{Mg^{2+}}}_{\mathrm{solv}}$, with reported experimental values.

All the computations used XSEDE SEAGrid. Science Gateway provided resources and services using the GridChem organization.[48−51]

RESULTS AND DISCUSSION

In this section, we present the energetics of the first hydration shell and its structure and we discuss the equilibrium structures of calcium carbonate and the surrounding water molecules. We also present free energies of solvation and discuss the validity of the model.

The normalized difference between the zero-point energy corrected total energy (E) for each cluster and the corresponding total energy at the global minimum for each cluster size (E_{min}) is shown in Figure 3. The largest discrepancy is ∼0.0012%, which implies an energy difference smaller than ∼15 kcal/mol, suggesting that equilibrium structures with very similar energetics were obtained. For a cluster size smaller than 13 (n < 13), this difference is smaller than ∼7.5 kcal/mol.

The discrepancy between the zero-point energy corrected total energy of each structure and that of the global energy minimum for each cluster size increases with cluster size, as it becomes gradually more likely to converge to local energy minima. The magnitude of this discrepancy is common among structures generated using the B3LYP exchange functional, as reported for $Ca^{2+}{\cdot}nH_2O$ clusters before.[28] Considering the large number of optimized structures, the deviation between the calculated energies (<0.0012%) is acceptable. Structures generated with TINKER and optimized directly with Gaussian09 exhibit slightly smaller energy differences for 50% of the clusters.

A clear outlier is observed for n = 2 in Figure 3. This structure was generated using the MMFF TINKER force field and subsequently optimized with DFTB+ and Gaussian09, with the inset showing the resulting structure. For this particular case, one of the two water molecules was not directly interacting with Ca^{2+} but rather with the CO_3^{2-}. As suggested by the large energy difference $(E - E_{\mathrm{min}})/E_{\mathrm{min}}$, this hydration

DOI: 10.1021/acs.jpca.5b09006
J. Phys. Chem. A 2015, 119, 11591−11600

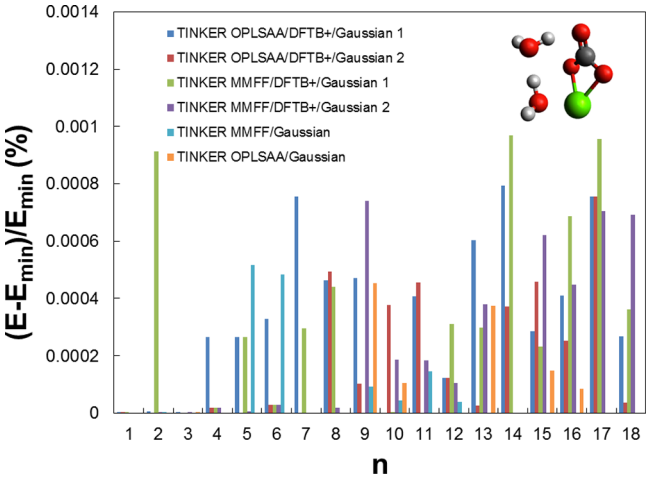

Figure 3. Difference of zero-point energy, E, for each cluster and the corresponding global energy minimum, E_{min}, for the cluster size (n). The legend gives the force field used to generate the initial cluster geometry (OPLS-AA or MMFF) and whether DFTB+ was used to optimize TINKER structures before final Gaussian09 optimization. The two lowest-energy geometries optimized with the same method are shown, denoted by Gaussian 1 and Gaussian 2. Inset: $CaCO_3 \cdot 2H_2O$ structure with the highest energy.

structure is less energetically favorable than the hydration structures where the two water molecules interact directly with Ca^{2+}. This is likely to result from the strong interaction between a single water molecule and Ca^{2+}, whereas the interaction between water and carbonate is weak.

The average binding energy between calcium carbonate and the surrounding water molecules, E_{avg} is given by[28,29]

$$E_{avg} = (E^{CaCO_3 \cdot nH_2O} - (E^{CaCO_3} + nE^{H_2O}))/n$$

where n is the number of water molecules in the optimized cluster, E^{CaCO_3} is the zero-point energy corrected total energy of a single calcium carbonate molecule, E^{H_2O} is the zero-point energy corrected total energy of a single water molecule, and $E^{CaCO_3 \cdot nH_2O}$ is the zero-point energy corrected total energy of the optimized cluster. The incremental binding energy is defined as[29]

$$\Delta E = E^{CaCO_3 \cdot nH_2O} - (E^{CaCO_3 \cdot (n-1)H_2O} + E^{H_2O})$$

i.e. it gives the change of the binding energy caused by the addition of one water molecule to the cluster. Similarly, the incremental binding free energy is obtained from

$$\Delta G = G^{CaCO_3 \cdot nH_2O} - (G^{CaCO_3 \cdot (n-1)H_2O} + G^{H_2O})$$

Negative values of ΔG indicate that addition of one water molecule to the cluster is thermodynamically favorable, i.e. spontaneous. The free energy term $G^{CaCO_3 \cdot nH_2O}$ corresponds to the ab initio free energy of the gas-phase clusters (upper right corner of the thermodynamic cycle in Figure 2).

Incremental addition of water molecules to the system (hydration) decreases the average binding energy of the cluster, as shown by the less negative average binding energy E_{avg} with increasing cluster size in Figure 4a. Concurrently, the hydrogen bond network of water within the first hydration shell becomes less influenced by the interactions with calcium carbonate with an increase in cluster size, as demonstrated later. The discrepancy between the calculated binding energies with the two selected optimization methods (B3LYP and MP2) is also shown in Figure 4a; MP2 leads to consistently more negative binding energies (~3 kcal/mol) but the trends are similar.

The incremental binding energy ΔE during hydration becomes less negative with increasing cluster size (Figure 4b), and it seems to achieve a plateau at $n > 11$. This indicates an almost constant energy gain for the addition of a water molecule for a cluster size larger than ~11, and as shown later, it coincides with the formation of the second hydration shell of calcium carbonate. Finally, the incremental binding free energy, ΔG, also becomes less negative with increasing cluster size (Figure 5). A negative binding free energy indicates that cluster formation is favorable or spontaneous. According to these results, ΔG tends to zero with increasing cluster size n, and hydrated clusters larger than $n \sim 15$ are not thermodynamically favorable (note the small positive values for ΔG at $n > 15$).

Probability density functions (PDFs) were computed using the obtained distances for $Ca-O_w$ and O_c-H_w pairs (see Figure 1 for the nomenclature) for the lowest-energy equilibrium clusters. The coordination number of calcium and carbonate oxygen was determined using the distance r at the first minimum of the PDF as the interaction cutoff distance (see red arrows in Figure 6b). Water molecules, whose atoms were within this cutoff distance, were considered to interact directly with either calcium (Ca) or carbonate oxygens (O_c) and to be

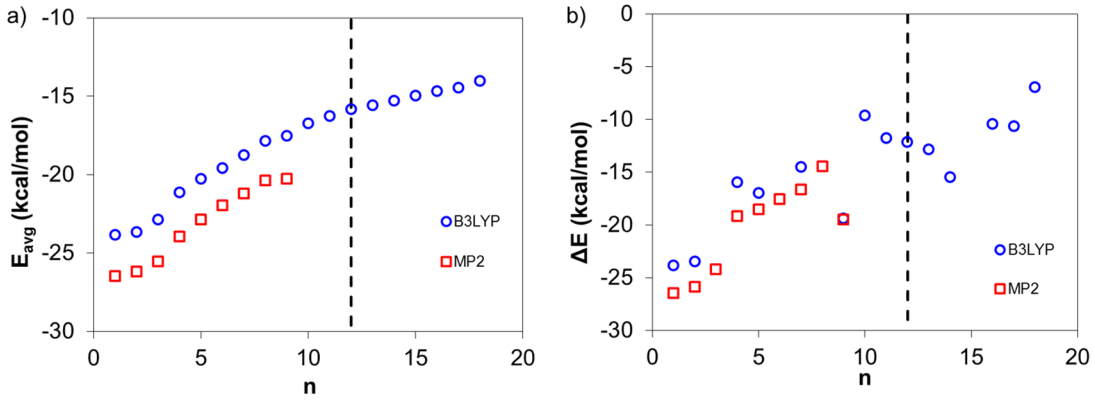

Figure 4. (a) Average binding energies for $CaCO_3 \cdot nH_2O$ clusters per mol of water upon hydration (E_{avg}) for the lowest-energy structures as a function of the cluster size. (b) Incremental binding energies upon hydration (ΔE) for the lowest-energy structures as a function of the cluster size. Dotted line shows the cluster size to complete the 1st hydration shell (n = 12).[29]

DOI: 10.1021/acs.jpca.5b09006
J. Phys. Chem. A 2015, 119, 11591−11600

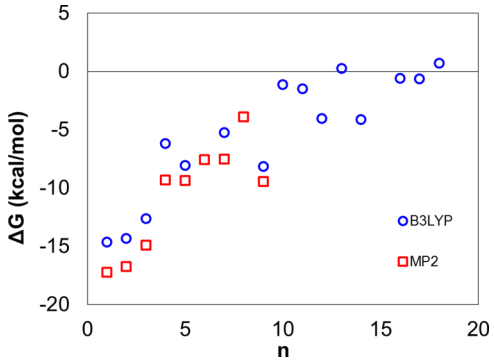

Figure 5. Incremental binding free energies for $CaCO_3{\cdot}nH_2O$ clusters, ΔG, using structures optimized with TINKER/DFTB+/Gaussian09. The diagram shows the results for the lowest-energy structures as a function of the cluster size.

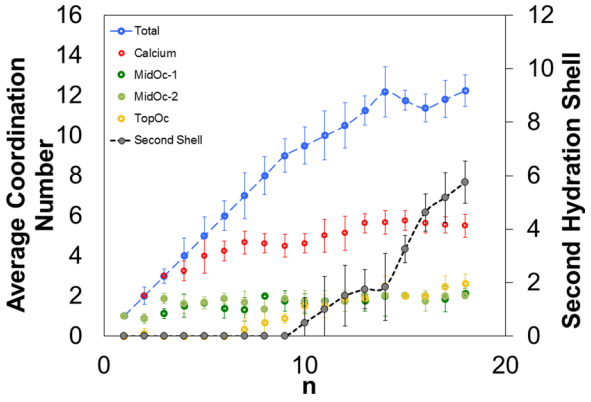

Figure 7. Average coordination number of $CaCO_3$ (total), calcium, bridging oxygen atoms (Mid-O_c), and nonbridging oxygen atom (Top-O_c) in the first hydration shell (left *Y*-axis), and coordination number in the second hydration shell (right *Y*-axis) as a function of the cluster size. Average values were obtained with the coordination numbers obtained for the optimized structures at each cluster size. The first minimum of the computed PDFs was used to determine cutoff distances and resulting coordination numbers.

part of the hydration shell. The cutoff distances for all cluster sizes were smaller than 3.4 Å for Ca−O_w and than 2.4 Å for O_c−H_w.

The average coordination number of each atom in the calcium carbonate cluster and the total average coordination number of the molecule are shown in Figure 7 as a function of cluster size. In agreement with reported values,[23,53] calcium can coordinate an average of 5.5 water molecules. Our results show that the "top" oxygen (Top-O_c) in carbonate does not interact with water molecules until the cluster size reaches a size of n = 7, and it coordinates an average of 2.6 water molecules at n = 18. The coordination number of calcium carbonate is ∼12 water molecules in its first hydration shell. For the largest investigated computed cluster size (n = 18), 12 water molecules can coordinate directly with calcium carbonate, and the other 6 water molecules are part of the second hydration shell. However, we note an inflection point for the average coordination number in the second hydration at n ∼ 15 that coincides with the hydration numbers at which $\Delta G \geq 0$ (Figure 6), i.e. for clusters that are not thermodynamically stable.

The computed cluster structures show the preferred sites occupied by water molecules around calcium carbonate (see Optimized Structures for $CaCO_3{\cdot}nH_2O$ in Supporting Information). Water molecules coordinating directly with Ca^{2+} were oriented with the water oxygen pointing toward calcium carbonate. Conversely, water molecules engaging in hydrogen bonding with CO_3^{2-} were oriented with the hydrogen atom toward calcium carbonate, as expected. MD simulations in ref 23 led to an extra molecule in the first hydration shell of calcium carbonate; however, although Bruneval et al. reported that the carbonate oxygen opposite to calcium (Top-O_c) could

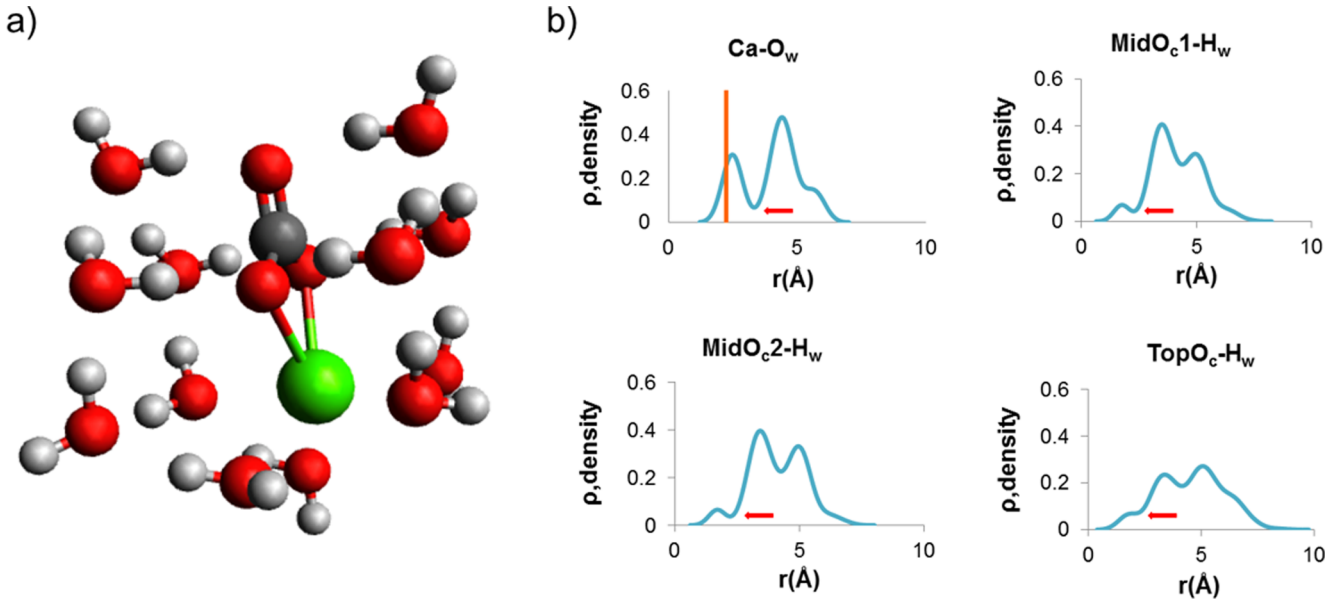

Figure 6. (a) Optimized geometry for a $CaCO_3{\cdot}12H_2O$ cluster (total energy $E = -1.17 \times 10^6$ kcal/mol) at the B3LYP/6-311G(d,p) level. Color legend: calcium (green), carbon (gray), oxygen (red), hydrogen (white), water oxygen (red), water hydrogen (white). Oxygen and hydrogen in water are denoted by subscript *w*. (b) PDFs for Ca−O_w, Mid-O_c1−H_w, Mid-O_c2−H_w, and Top-O_c−H_w distances in $CaCO_3{\cdot}12H_2O$. Red arrows show the first minimum in the PDF. Orange line in Ca−O_w shows the average Ca−O_w distance at the calcite−water interface (2.248 Å) for comparison.[52]

DOI: 10.1021/acs.jpca.5b09006
J. Phys. Chem. A 2015, 119, 11591−11600

form up to four hydrogen bonds with water, our simulations show a maximum of three hydrogen bonds. Our ab initio-level calculations show that it is more favorable for this water molecule to step out on to the second hydration shell instead of fully coordinating the top carbonate oxygen in the first hydration shell. As a result, the coordination number of the first hydration shell of calcium carbonate is 12.

Figure 8 shows that the length of the Ca−O_c bond increases with the number of water molecules in the hydration shell,

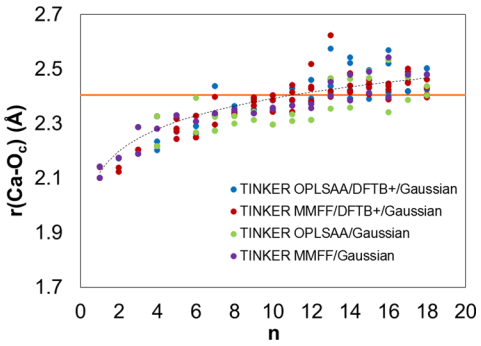

Figure 8. Length of Ca−O_c bond. Legend indicates the force field used to generate the initial cluster geometry (OPLS-AA or MMFF) and whether DFTB+ was used to optimize TINKER structures before final Gaussian09 optimization. Orange line indicates the average Ca−O_c bond length at the calcite−water interface.[52]

consistent with the partial screening of the Coulombic interaction between the ions. The observed bond lengths for $n > 9$ are similar to those observed for the Ca−O_c bond at the calcite-water interface, which ranges from 2.305 to 2.585 Å.[52] Natural bond orbitals (NBO)-derived atomic charges of the calcium carbonate clusters show a decrease of the positive charge on calcium and of the negative charge on the carbonate oxygen atoms (O_c) as a function of the cluster size (see Figure SM2 in Supporting Information). This variation indicates a slight decrease in the strength of the (ionic) Ca−O_c bond that is consistent with the observed bond elongation in Figure 8. The strong association of calcium with carbonate ions, albeit slightly reduced ionic interactions, is consistent with the low solubility of calcium carbonate and the large free energy barrier for dissociation at room temperature (~8 kcal/mol in ref 23).

The observed increase in bond length with increasing cluster size correlates with the decrease in the average binding energy of the clusters, i.e. with E_{avg} becoming less negative (Figure 4). Besides, the plateau of the incremental binding energy ΔE at $n > 11$ is achieved as water molecules start occupying the second hydration shell (Figure 7, right *Y*-axis). Thus, the thermodynamic calculations are consistent with the intramolecular structural analysis and PDFs.

Out-of-plane bending of a calcium carbonate molecule (i.e., Ca−C−Top−O_c angles <180°) was observed for most isomers at each cluster size (see Figure SM3 in Supporting Information), although it has been shown to have energetic penalties.[23,26,39,54,55] Our simulations demonstrate that low energy $CaCO_3{\cdot}nH_2O$ structures can be achieved despite the large bending of the molecule, as a result of the favorable hydration of the calcium carbonate molecule. This suggests that out-of-plane bending of the calcium carbonate molecule does not have a dominant effect on the total energy of a solvated calcium carbonate molecule and the gain in energy by the water−calcium carbonate interactions can overcome the energy penalty for the bending.

We also investigated the structural parameters of the hydration shell. Reported bond lengths of a free water molecule ($r(O_w{-}H_w)$, see Figure 1) range from 0.957 to 0.970 Å and bond angles of water ($H_w{-}O_w{-}H_w$, see Figure 1) are between 104.2° and 105.1°.[56,57] Bond lengths and angles for water molecules in the lowest energy structure, at each cluster size, are shown in Figure 9a,b, respectively; average values for all water molecules interacting with calcium carbonate (and resulting standard deviation) are calculated at each cluster size. We consider two bond lengths $r(O_w{-}H_w)$ for each water molecule (i.e., for the two hydrogen atoms); the average bond length of the water molecules directly interacting with either Ca^{2+} or CO_3^{2-} differ significantly from those of the free water molecule (upper curves with circles in Figure 9a), whereas the length of the second bond is close to that of bulk water (lower curves with squares in Figure 9a tend to ~0.96−0.97 Å). The water molecules in the second hydration shell are shown separately (blue symbols). As the number of water molecules in the hydration shell *n* increases, both, average bond length and angle (Figure 9b) tend toward those of bulk water, meaning that the hydrogen bond network between the water molecules in the first hydration shell becomes less influenced by the

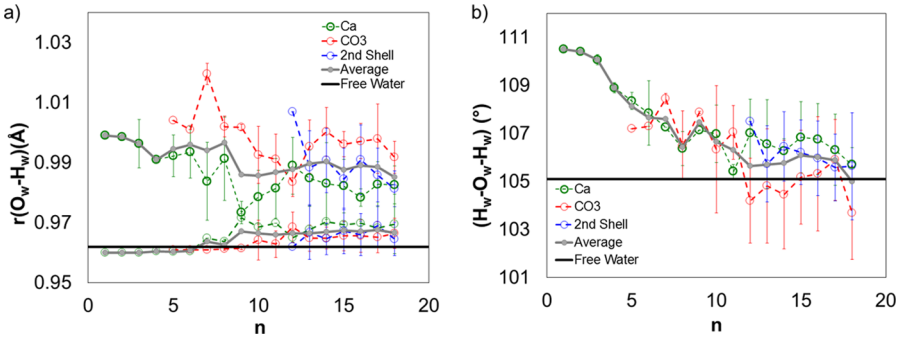

Figure 9. (a) Average ($O_w{-}H_w$) bond lengths for water molecules interacting with Ca^{2+} (green), with O_c (red), and the average (gray) in the 1st hydration shell, and average bond lengths of the water molecules in the second hydration (blue). The circles give the bond length of one of the two ($O_w{-}H_w$) bonds—the one that interacts more strongly with calcium carbonate—and the squares for the other bond in the water molecule. (b) Average bond angles ($H_w{-}O_w{-}H_w$) for water molecules interacting with Ca^{2+} (green), O_c (red), and the average (gray) in the 1st hydration shell, and average bond angles of the water molecules in the second hydration shell (blue). Free water molecule bond length $O_w{-}H_w$ (a) and $H_w{-}O_w{-}H_w$ angle (b) are given by the black lines.

DOI: 10.1021/acs.jpca.5b09006
J. Phys. Chem. A 2015, 119, 11591−11600

Table 1. Calculated Free Energy of Solvation of $CaCO_3{\cdot}nH_2O$ ($\Delta G^{*CaCO_3}_{solv}$), Free Energy of Gas-Phase Cluster ($\Delta G^{CaCO_3{\cdot}nH_2O}_{clust}$), Free Energy of the Hydrated Cluster from Gas to Liquid ($\Delta G^{*CaCO_3{\cdot}nH_2O}_{gl}$), and Vaporization Free Energy of n Water Molecules ($n\Delta G^{H_2O}_{vap}$)

	$\Delta G^{CaCO_3{\cdot}nH_2O}_{clust}$		$\Delta G^{*CaCO_3{\cdot}nH_2O}_{gl}$		$n\Delta G^{H_2O}_{vap}$		$\Delta G^{*CaCO_3}_{solv}$	
n	B3LYP	MP2	B3LYP	MP2	B3LYP	MP2	B3LYP	MP2
1	−14.7	−17.2	−73.1	−80.6	0.8	0.8	−87.0	−97.0
2	−28.9	−34.0	−59.4		1.5	1.7	−86.8	
3	−41.3	−48.9	−48.8		2.3	2.5	−87.8	
4	−47.5	−58.2	−42.5	−44.1	3.1	3.3	−86.9	−99.0
5	−55.6	−67.6	−37.8	−41.6	3.9	4.2	−89.5	−105.1
6	−61.4	−75.2	−34.8	−39.6	4.6	5.0	−91.5	−109.9
7	−65.7	−82.7	−34.6	−37.3	5.4	5.8	−94.9	−114.2
8	−67.4	−86.7	−29.9		6.2	6.6	−91.2	
9	−70.6	−96.2	−25.4		7.0	7.5	−89.1	
10	−71.4		−27.3		7.7		−90.9	
11	−73.5		−27.2		8.5		−92.1	
12	−73.3		−28.0		9.3		−92.0	
13	−77.3		−27.7		10.1		−95.0	
14	−77.5		−28.4		10.8		−95.1	
15	−78.8		−26.9		11.6		−94.2	
16	−79.5		−27.9		12.4		−95.0	
17	−80.1		−27.7		13.2		−94.6	
18	−79.5		−30.0		13.9		−95.5	

Table 2. Calculated Free Energy of Solvation ΔG^{*s}_{solv} of Two Different Solutes, S = Ca^{2+} or S = Mg^{2+}, and Their Comparison to Experimental and Computational Literature Values

	ΔG^{*s}_{solv}			
S	B3LYP/6-311+G(d,p)	MP2/6-311+G(d,p)	exptl[58]	PBE-DNP COSMO[35]
Ca^{2+}	−360.31	−364.42	−381.6	−352.7
Mg^{2+}	−432.57	−431.37	−455.5	−438.8

interactions with calcium carbonate. The standard variation for both, bond length and angle of the water molecules becomes significant for $n > 10$, suggesting a significant variability in the interactions of the coordinating water molecules with calcium carbonate.

To the best of our knowledge, free energies of solvation of calcium carbonate in basic conditions have not been reported yet. The bulk solvation of the $CaCO_3{\cdot}nH_2O$ clusters in water was performed using the PCM model, and the results are summarized in Table 1. The lowest-energy gas phase clusters were reoptimized within the PCM water solvent model at a B3LYP/6-311G(d,p) level of theory. Selected structures were also optimized using the PCM model at the MP2/6-311G(d,p) level. No standard deviation is reported since at most two structures were optimized for each cluster size n.

Our computations yield that the solvation free energy of calcium carbonate ranges from −87.0 kcal/mol to −95.5 kcal/mol, becoming more negative with increasing cluster size; above $n > 13$ the variation of the solvation free energy is very small (−94.2 to −95.5 kcal/mol), consistent with the negligible incremental free energy ΔG for such large clusters. Hydration does not imply bond dissociation, as discussed before. Experimental values for the solvation free energy for comparison to our calculated values were not found. Calculated values for Ca^{2+} and Mg^{2+} with their full first hydration shell using the same basis set and DFT methods as for the $CaCO_3{\cdot}nH_2O$ clusters are shown in Table 2 to evaluate the reliability of the method. The calculated free energies of solvation for $Ca^{2+}{\cdot}6H_2O$ and $Mg^{2+}{\cdot}6H_2O$ are in good agreement with previous experimental and computational results.[35,47] These results demonstrate that the continuum PCM model is adequate to calculate the free energy of hydration of ions, and that the developed methodology, the selected DFT method and basis set provide accurate thermodynamic quantities. Based on these results, ab initio quantum chemistry methods could be a powerful tool to study the structure and thermodynamics of PNCs and critical nuclei in the calcium carbonate mineralization pathway.

Bidentate and monodentate binding arrangements are relevant in calcium carbonate polymorphs: e.g. the bidentate binding arrangement is present in monohydrate calcite and aragonite,[59] whereas the monodentate structure can become a significant fraction of the two coordination modes observed in other calcium carbonate polymorphs, including the amorphous phase(∼55%).[60] Both computational and experimental studies have shown that Ca^{2+} can bind in both monodentate and bidentate coordination with CO_3^{2-}.[11,15,35,53,59,60] In contrast, and despite the extensive conformational searches performed in this work, solely the bidentate binding motif was found in the obtained equilibrium calcium carbonate structures. It is notable that some simulations were initiated with a monodentate structure, but a bidentate arrangement was obtained after optimization. Single-molecule MD simulations also lead to a tightly bound bidentate structure, in agreement with our results.[23] This is an interesting result that suggests that single-molecule simulations could promote the existence of the bidentate $CaCO_3$ structure, whereas the probability of monodentate structures increases as more molecules are considered in simulations. The occurrence of these binding motifs results from a complex balance between the interactions

DOI: 10.1021/acs.jpca.5b09006
J. Phys. Chem. A 2015, 119, 11591−11600

of the ions and the surrounding water molecules, and the actual thermodynamic behavior is a long-term average, out of reach for many computational techniques.[61] Several works have shown that the energy barrier between bidentate and monodentate structures is small, which allows facile conversion between the two states.[11,15,35,61] For charged hydrated calcium bicarbonate clusters with n = 1 and 2, the bidentate arrangement is preferred, whereas for n = 3, 4, and 5, the monodentate motif is more stable by ∼3 kcal/mol.[35] We attribute the discrepancy between these and our results to the lower ionic character of the bicarbonate ion, and to the resulting weaker interactions between Ca^{2+} and bicarbonate, compared to those present for the carbonate used in our simulations. This is supported by Raitieri and Gale's studies at a shared free energy well that showed the bidentate structure to be more stable at shorter $Ca-O_c$ distances, and the monodentate to be stabilized at longer bond lengths, i.e. for weaker interactions between calcium and oxygen atoms,[11] and also by more recent MD simulations with a new force field for alkaline Earth carbonates.[30] Therefore, the favored stabilization of the bidentate motif in our ab initio study of a single calcium carbonate molecule is the result of the strong interaction between calcium and carbonate. Given the widespread presence of bidentate ligands in many calcium carbonate systems, our approach is of relevance to the study of calcium carbonate hydration.

CONCLUSIONS

In this work, we present a new methodology to study the hydration shell and equilibrium structures of large hydrated clusters, using a combination of molecular mechanics, Density Functional based Tight Binding method simulations, and ab initio simulations. Structural analysis of a single calcium carbonate molecule reveals a total coordination of 12 water molecules and a change of the structure of the water molecules in the first hydration shell owing to strong interactions with calcium carbonate. Our analysis indicates that hydrated clusters with more than 15 water molecules are not thermodynamically favorable. Finally, a continuum model was used to estimate the free energy of hydration of calcium carbonate, and values ranging from −87 kcal/mol to −95 kcal/mol were obtained.

ASSOCIATED CONTENT

Supporting Information

The Supporting Information is available free of charge on the ACS Publications website at DOI: 10.1021/acs.jpca.5b09006.

Additional information on the number of structures generated with TINKER, NBO charges and bond angles, a list of the optimized structures for n = 1−18 and their corresponding energies (PDF)

AUTHOR INFORMATION

Corresponding Author

*E-mail: rosae@illinois.edu.

Notes

The authors declare no competing financial interest.

ACKNOWLEDGMENTS

This material is based upon work supported by the National Science Foundation Graduate Research Fellowship under Grant No. CMMI-1435920. We also thank the National Center for Supercomputing Applications (NCSA) for financial support for Yijue Diao, and computing resources. We acknowledge Maximilian Kubillus at the Elstner's group in the Karlsruhe Institute of Technology for providing us with a new set of DFTB+ parameters.

REFERENCES

(1) Li, Q.; Fernandez-Martinez, A.; Lee, B.; Waychunas, G. A.; Jun, Y.-S. Interfacial Energies for Heterogeneous Nucleation of Calcium Carbonate on Mica and Quartz. *Environ. Sci. Technol.* **2014**, *48*, 5745−5753.

(2) Radha, A. V.; Forbes, T. Z.; Killian, C. E.; Gilbert, P. U. P. A.; Navrotsky, A. Transformation and crystallization energetics of synthetic and biogenic amorphous calcium carbonate. *Proc. Natl. Acad. Sci. U. S. A.* **2010**, *107*, 16438−16443.

(3) Addadi, L.; Raz, S.; Weiner, S. Taking advantage of disorder: Amorphous calcium carbonate and its roles in biomineralization. *Adv. Mater.* **2003**, *15*, 959−970.

(4) Aizenberg, J.; Tkachenko, A.; Weiner, S.; Addadi, L.; Hendler, G. Calcitic microlenses as part of the photoreceptor system in brittlestars. *Nature* **2001**, *412*, 819−822.

(5) Lee, K.; Wagermaier, W.; Masic, A.; Kommareddy, K. P.; Bennet, M.; Manjubala, I.; Lee, S.-W.; Park, S. B.; Cölfen, H.; Fratzl, P. Self-assembly of amorphous calcium carbonate microlens arrays. *Nat. Commun.* **2012**, *3*, 725.

(6) Addadi, L.; Weiner, S. Biomineralization: mineral formation by organisms. *Phys. Scr.* **2014**, *89*, 098003.

(7) Cunningham, A. B.; Phillips, A. J.; Troyer, E.; Lauchnor, E.; Hiebert, R.; Gerlach, R.; Spangler, L. Wellbore leakage mitigation using engineered biomineralization. *Energy Procedia* **2014**, *63*, 4612−4619.

(8) Phillips, A. J.; Lauchnor, E.; Eldring, J.; Esposito, R.; Mitchell, A. C.; Gerlach, R.; Cunningham, A. B.; Spangler, L. H. Potential CO2 Leakage Reduction through Biofilm-Induced Calcium Carbonate Precipitation. *Environ. Sci. Technol.* **2013**, *47*, 142−149.

(9) Li, Q.; Csetenyi, L.; Gadd, G. M. Biomineralization of Metal Carbonates by Neurospora crassa. *Environ. Sci. Technol.* **2014**, *48*, 14409−14416.

(10) Yang, Q.; Liu, Y.; Gu, A.; Ding, J.; Shen, Z. Investigation of Calcium Carbonate Scaling Inhibition and Scale Morphology by AFM. *J. Colloid Interface Sci.* **2001**, *240*, 608−621.

(11) Raiteri, P.; Gale, J. D. Water Is the Key to Nonclassical Nucleation of Amorphous Calcium Carbonate. *J. Am. Chem. Soc.* **2010**, *132*, 17623−17634.

(12) Nebel, H.; Neumann, M.; Mayer, C.; Epple, M. On the Structure of Amorphous Calcium Carbonate—A Detailed Study by Solid-State NMR Spectroscopy. *Inorg. Chem.* **2008**, *47*, 7874−7879.

(13) Dorvee, J. R.; Veis, A. Water in the formation of biogenic minerals: peeling away the hydration layers. *J. Struct. Biol.* **2013**, *183*, 278−303.

(14) Gebauer, D.; Kellermeier, M.; Gale, J. D.; Bergstrom, L.; Colfen, H. Pre-nucleation clusters as solute precursors in crystallisation. *Chem. Soc. Rev.* **2014**, *43*, 2348−2371.

(15) Tribello, G. A.; Bruneval, F.; Liew, C.; Parrinello, M. A molecular dynamics study of the early stages of calcium carbonate growth. *J. Phys. Chem. B* **2009**, *113*, 11680−11687.

(16) Quigley, D.; Rodger, P. M. Free energy and structure of calcium carbonate nanoparticles during early stages of crystallization. *J. Chem. Phys.* **2008**, *128*, 221101.

(17) Quigley, D.; Rodger, P. M.; Freeman, C.; Harding, J.; Duffy, D. Metadynamics simulations of calcite crystallization on self-assembled monolayers. *J. Chem. Phys.* **2009**, *131*, 094703.

(18) Freeman, C. L.; Harding, J. H.; Quigley, D.; Rodger, P. M. Structural control of crystal nuclei by an eggshell protein. *Angew. Chem., Int. Ed.* **2010**, *49*, 5135−5137.

(19) Richens, D. T. *The Chemistry of Aqua Ions: Synthesis, Structure and Reactivity: A Tour Through the Periodic Table of the Elements*; Wiley: New York, 1997.

DOI: 10.1021/acs.jpca.5b09006
J. Phys. Chem. A 2015, 119, 11591−11600

(20) Bogatko, S.; Cauët, E.; Bylaska, E.; Schenter, G.; Fulton, J.; Weare, J. The Aqueous Ca2+ System, in Comparison with Zn2+, Fe3 + , and Al3 + : An Ab Initio Molecular Dynamics Study. *Chem. - Eur. J.* **2013**, *19*, 3047−3060.
(21) Ikeda, T.; Boero, M.; Terakura, K. Hydration properties of magnesium and calcium ions from constrained first principles molecular dynamics. *J. Chem. Phys.* **2007**, *127*, 074503.
(22) Gebauer, D.; Völkel, A.; Cölfen, H. Stable Prenucleation Calcium Carbonate Clusters. *Science* **2008**, *322*, 1819−1822.
(23) Bruneval, F.; Donadio, D.; Parrinello, M. Molecular dynamics study of the solvation of calcium carbonate in water. *J. Phys. Chem. B* **2007**, *111*, 12219−12227.
(24) Kumar, P. P.; Kalinichev, A. G.; Kirkpatrick, R. J. Hydrogen-Bonding Structure and Dynamics of Aqueous Carbonate Species from Car−Parrinello Molecular Dynamics Simulations. *J. Phys. Chem. B* **2009**, *113*, 794−802.
(25) Leung, K.; Nielsen, I. M. B.; Kurtz, I. Ab Initio Molecular Dynamics Study of Carbon Dioxide and Bicarbonate Hydration and the Nucleophilic Attack of Hydroxide on CO2. *J. Phys. Chem. B* **2007**, *111*, 4453−4459.
(26) Dang, L. X.; Smith, D. E. Comment on "Mean force potential for the calcium−chloride ion pair in water" [J. Chem. Phys. 99, 4229 (1993)]. *J. Chem. Phys.* **1995**, *102*, 3483−3484.
(27) Di Tommaso, D.; Ruiz-Agudo, E.; de Leeuw, N. H.; Putnis, A.; Putnis, C. V. Modelling the effects of salt solutions on the hydration of calcium ions. *Phys. Chem. Chem. Phys.* **2014**, *16*, 7772−85.
(28) Lei, X. L.; Pan, B. C. Structures, Stability, Vibration Entropy and IR Spectra of Hydrated Calcium Ion Clusters [Ca(H2O)n]2+ (n = 1−20, 27): A Systematic Investigation by Density Functional Theory. *J. Phys. Chem. A* **2010**, *114*, 7595−7603.
(29) Zhao, Y.-L.; Meot-Ner, M.; Gonzalez, C. Ionic Hydrogen-Bond Networks and Ion Solvation. 1. An Efficient Monte Carlo/Quantum Mechanical Method for Structural Search and Energy Computations: Ammonium/Water. *J. Phys. Chem. A* **2009**, *113*, 2967−2974.
(30) Raiteri, P.; Demichelis, R.; Gale, J. D. A Thermodynamically Consistent Force Field for Molecular Dynamics Simulations of Alkaline-Earth Carbonates and Their Aqueous Speciation. *J. Phys. Chem. C* **2015**, *119*, 24447.
(31) Mahadevan, T. S.; Garofalini, S. H. Dissociative water potential for molecular dynamics simulations. *J. Phys. Chem. B* **2007**, *111*, 8919−8927.
(32) Demichelis, R.; Raiteri, P.; Gale, J. D.; Quigley, D.; Gebauer, D. Stable prenucleation mineral clusters are liquid-like ionic polymers. *Nat. Commun.* **2011**, *2*, 590.
(33) Gale, J. D.; Raiteri, P.; van Duin, A. C. T. A reactive force field for aqueous-calcium carbonate systems. *Phys. Chem. Chem. Phys.* **2011**, *13*, 16666−16679.
(34) Stefanovich, E. V.; Boldyrev, A. I.; Truong, T. N.; Simons, J. Ab initio study of the stabilization of multiply charged anions in water. *J. Phys. Chem. B* **1998**, *102*, 4205−4208.
(35) Tommaso, D. D.; de Leeuw, N. H. The Onset of Calcium Carbonate Nucleation: A Density Functional Theory Molecular Dynamics and Hybrid Microsolvation/Continuum Study. *J. Phys. Chem. B* **2008**, *112*, 6965−6975.
(36) Koga, N.; Yamane, Y. Thermal behaviors of amorphous calcium carbonates prepared in aqueous and ethanol media. *J. Therm. Anal. Calorim.* **2008**, *94*, 379−387.
(37) Ponder, J. W. *TINKER: Software tools for molecular design*, Version 6.3.3; Washington University School of Medicine: Saint Louis, MO, 2004.
(38) Freeman, C. L.; Harding, J. H.; Cooke, D. J.; Elliott, J. A.; Lardge, J. S.; Duffy, D. M. New Forcefields for Modeling Biomineralization Processes. *J. Phys. Chem. C* **2007**, *111*, 11943−11951.
(39) Raiteri, P.; Gale, J. D.; Quigley, D.; Rodger, P. M. Derivation of an Accurate Force-Field for Simulating the Growth of Calcium Carbonate from Aqueous Solution: A New Model for the Calcite−Water Interface. *J. Phys. Chem. C* **2010**, *114*, 5997−6010.
(40) Aradi, B.; Hourahine, B.; Frauenheim, T. DFTB+, a sparse matrix-based implementation of the DFTB method. *J. Phys. Chem. A* **2007**, *111*, 5678−5684.
(41) Eyert, V. A Comparative Study on Methods for Convergence Acceleration of Iterative Vector Sequences. *J. Comput. Phys.* **1996**, *124*, 271−285.
(42) Kubillus, M.; Kubař, T.; Gaus, M.; Řezáč, J.; Elstner, M. Parameterization of the DFTB3Method for Br, Ca, Cl, F, I, K, and Na in Organic and Biological Systems. *J. Chem. Theory Comput.* **2015**, *11*, 332−342.
(43) Frisch, M. J.; Trucks, G. W.; Schlegel, H. B.; Scuseria, G. E.; Robb, M. A.; Cheeseman, J. R.; Scalmani, G.; Barone, V.; Mennucci, B.; Petersson, G. A., et al. *Gaussian 09*; Gaussian, Inc.: Wallingford, CT, 2009.
(44) Foster, J.; Weinhold, F. Natural hybrid orbitals. *J. Am. Chem. Soc.* **1980**, *102*, 7211−7218.
(45) Reed, A. E.; Weinstock, R. B.; Weinhold, F. Natural population analysis. *J. Chem. Phys.* **1985**, *83*, 735−746.
(46) Head-Gordon, M.; Pople, J. A.; Frisch, M. J. MP2 energy evaluation by direct methods. *Chem. Phys. Lett.* **1988**, *153*, 503−506.
(47) Pliego, J. R.; Riveros, J. M. The Cluster−Continuum Model for the Calculation of the Solvation Free Energy of Ionic Species. *J. Phys. Chem. A* **2001**, *105*, 7241−7247.
(48) Shen, N.; Fan, Y.; Pamidighantam, S. E-science infrastructures for molecular modeling and parametrization. *Journal of Computational Science* **2014**, *5*, 576−589.
(49) Dooley, R.; Milfeld, K.; Guiang, C.; Pamidighantam, S.; Allen, G. From Proposal to Production: Lessons Learned Developing the Computational Chemistry Grid Cyberinfrastructure. *J. Grid Computing* **2006**, *4*, 195−208.
(50) Dooley, R.; Allen, G.; Pamidighantam, S. Computational chemistry grid: production cyberinfrastructure for computational chemistry. *Proceedings of the 13th Annual Mardi Gras Conference*, Louisiana State University, Baton Rouge, Lousiana, February 3−5, 2005.
(51) Milfeld, K.; Guiang, C.; Pamidighantam, S.; Giuliani, J. Cluster computing through an application-oriented computational chemistry Grid. *Proceedings of the 6th International Conference on Linux Clusters: The HPC Revolution*, University of North Carolina, Chapel Hill, North Carolina, April 26−28, 2005.
(52) Fenter, P.; Sturchio, N. C. Calcite (1 0 4)−water interface structure, revisited. *Geochim. Cosmochim. Acta* **2012**, *97*, 58−69.
(53) Di Tommaso, D.; de Leeuw, N. H. First Principles Simulations of the Structural and Dynamical Properties of Hydrated Metal Ions Me2+ and Solvated Metal Carbonates (Me = Ca, Mg, and Sr). *Cryst. Growth Des.* **2010**, *10*, 4292−4302.
(54) Saharay, M.; Yazaydin, A. O.; Kirkpatrick, R. J. Dehydration-induced amorphous phases of calcium carbonate. *J. Phys. Chem. B* **2013**, *117*, 3328−36.
(55) Thackeray, D. J.; Siders, P. D. Molecular-orbital and empirical-potential descriptions of CaCO3. *J. Chem. Soc., Faraday Trans.* **1998**, *94*, 2653−2661.
(56) Xu, X.; Goddard, W. A. Bonding Properties of the Water Dimer: A Comparative Study of Density Functional Theories. *J. Phys. Chem. A* **2004**, *108*, 2305−2313.
(57) Carl, D. R.; Moision, R. M.; Armentrout, P. B. Binding energies for the inner hydration shells of Ca2+: An experimental and theoretical investigation of Ca2+(H2O)x complexes (x = 5−9). *Int. J. Mass Spectrom.* **2007**, *265*, 308−325.
(58) Rosseinsky, D. R. Electrode Potentials and Hydration Energies. Theories and Correlations. *Chem. Rev.* **1965**, *65*, 467−490.
(59) Michel, F. M.; MacDonald, J.; Feng, J.; Phillips, B. L.; Ehm, L.; Tarabrella, C.; Parise, J. B.; Reeder, R. J. Structural Characteristics of Synthetic Amorphous Calcium Carbonate. *Chem. Mater.* **2008**, *20*, 4720−4728.
(60) Goodwin, A. L.; Michel, F. M.; Phillips, B. L.; Keen, D. A.; Dove, M. T.; Reeder, R. J. Nanoporous Structure and Medium-Range Order in Synthetic Amorphous Calcium Carbonate. *Chem. Mater.* **2010**, *22*, 3197−3205.

DOI: 10.1021/acs.jpca.5b09006
J. Phys. Chem. A 2015, 119, 11591−11600

(61) Scott, L. *Reduced Calcium Carbonate Scaling Through Turbulent Physical Conditioning*. Ph.D. Thesis, University of Wollongong, New South Wales, Australia, 2012.

DOI: 10.1021/acs.jpca.5b09006
J. Phys. Chem. A 2015, 119, 11591−11600